Measurements of Magnetic Field Harmonics In Superconductor Coil Wound By Surface Winding Technology

Naoyuki Amemiya, Shingo Mizuta, Taketsune Nakamura, Toru Ogitsu, Tomofumi Orikasa, Tsutomu Kurusu, Tetsuhiro Obana, and Koji Noda

***Abstract*—Magnetic field harmonics (multi-pole component of magnetic field) were measured in a 24-layer coil for a dipole magnet wound with NbTi round wires by using the surface winding technology (direct winding technology). The coil was wound layer by layer, and the magnetic field measurements were carried out by using rotating pick-up coil system, when the 4 layers, 10 layers, 16 layers, 20 layers, and 24 layers of the coil were wound. The measured magnetic field harmonics were compared with theoretical values. The error, which is the difference between the measured value and theoretical one, does not increase substantially with increasing number of wound layers when measured at the center of the coil. Larger errors measured near the coil end should have been caused by the position errors of wires, which was observed visually.**

***Index Terms*—Accelerator magnets, direct winding, field harmonics, surface winding.**

I. Introduction

In beam-guiding magnets for particle accelerators, the generation of the precisely controlled magnetic field required by their functions is a very important issue. There are two types of such magnets: the coil-dominated magnet and iron-dominated magnet [1]. In the former, the precisely-designed positions of wires ensure the generation of the precise magnetic field. In the latter, the precisely-designed shape of the iron pole ensures the generation of the precise magnetic field. Superconducting magnets generating high magnetic fields are coil-dominated ones. The surface winding technology by using a 6 axis computer numerical controlled (CNC) winding machine developed by Toshiba is a novel technology to wind a superconductor coil for coil-dominated magnets [2], [3]. This technology is similar to the *direct wind* developed at BNL [4]–[6]. It enables to wind a coil with arbitrary wire positions to generate a specified magnetic field [2], [3], [7], [8].

In the surface winding technology by using a 6 axis CNC winding machine, a coil is wound layer by layer. One of the concerns in the magnets wound by using this technology is the accuracy of positioning wires. Ohuchi *et al.* constructed a test quadrupole consisting of two-layer coils by this type of winding method [8], and they cut the straight section of the test quadrupole perpendicularly to measure the positions of wires on the cross-section. They numerically calculated the magnetic field harmonics (multi-pole component of magnetic field, multi-pole coefficient) based on the measured positions of wires. In coils with many layers, the position errors might become more serious problem, because they might accumulate in the layer-by-layer winding process.

The objective of this study is to clarify experimentally the magnetic field accuracy of a coil wound by the surface winding technology by using a CNC winding machine. A 24-layer coil for a dipole magnet was constructed with a NbTi round wire, and its magnetic field harmonics were measured during its layer-by-layer winding process: they were measured after winding the fourth layer, the tenth layer, the sixteenth layer, the twentieth layer, and the twenty-fourth layer. The measured magnetic field harmonics were compared with the theoretical ones. The cross-sectional dimensions of the coil were also measured for discussion.

II. Winding Process And Constructed Superconductor Coil for Measurements

A. Winding Process

The surface winding technology based on CNC winding machine is as follows [2], [3]. One continuous round wire is place on an insulated mandrel as followed the designed position by using a computer controlled winding head, and it is bonded on the insulated mandrel with thermoplastic high polymer. An ultrasonic heater installed in the winding head is used to bond the wire. Once one layer of winding is completed, it is wrapped with a glass-fiber-reinforced-plastic (GFRP) sheet. Then, the next layer is wound on the wrapped and bonded GFRP sheet in the similar way.

Manuscript received 13 September 2011. This work was supported in part by the Japan Science and Technology Agency under the Strategic Promotion of Innovative Research and Development Program.

N. Amemiya, S. Mizuta and T. Nakamura are with Kyoto University, Kyoto 615-8510, Japan (phone: 81-75-383-2220; fax: 81-75-383-2224; e-mail: amemiya@kuee.kyoto-u.ac.jp).

T. Ogitsu is with High Energy Accelerator Research Organization, Tsukuba 305-0801, Japan (email: ogitsu@post.kek.jp).

T. Orikasa and T. Kurusu are with Toshiba Corporation, Tokyo 105-8001, Japan (email: tsutomu.kurusu@toshiba.co.jp).

T. Obana is with National Institute for Fusion Science, Toki 509-5292, Japan (obana.tetsuhiro@LHD.nifs.ac.jp).

K. Noda is with National Institute of Radiological Sciences, Chiba 263-8555, Japan (email: noda_k@nirs.go.jp).

TABLE I DIMENSIONS OF COIL

Total length	560 mm
Length of straight section	330 mm
Radius of mandrel	75 mm
Number of layers	26 (designed) 24 (wound for measurements)

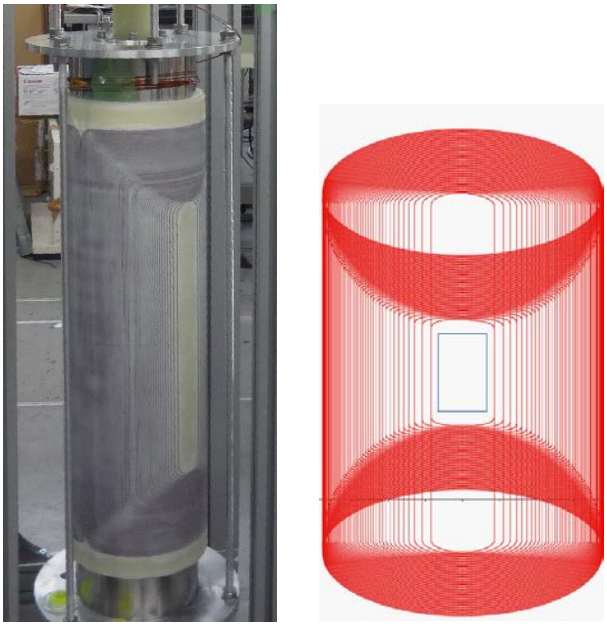

(a) (b)

Fig. 1. Constructed superconductor coil for measurements: (a) photograph of the coil, when it was wound to its 16 layers (b) designed position of wire in a layer of coil.

B. Constructed Superconductor Coil for Measurements

A 26-layer superconductor coil for a dipole magnet was designed, and up to 24 layers were wound for the magnetic field harmonics measurements. The dimensions of the coil are listed in Table I. Fig. 1(a) is a photograph of the coil, after winding the sixteenth layer. Fig. 1(b) shows the designed position of the wire in a layer.

III. EXPERIMENTAL AND THEORETICAL METHODS

A. Experimental Method

When measuring the magnetic field harmonics, the coil was placed in a cryostat and was cooled in liquid nitrogen to reduce the resistance of the NbTi wire, because the output voltage of the power supply used was limited. A rotating pick-up coil system was placed in the inner cryostat inserted into the bore of the magnet, and the magnetic field harmonics were measured. The schematic of the rotating pick-up coil system is shown in Fig. 2. It consists of three coils (A, B, C) patterned on a plastic plate. The rotating axis locates at the center of the coil B. Its entire width and length are 26 mm and 120 mm, respectively. The coil A and the coil B were connected in series so as to cancel the dipole component and to detect higher harmonics. The coil C was used independently to detect the all harmonics including the dipole component.

Here, z coordinate is set along the superconductor coil axis, and its origin is set at its center. The position of the pick-up coil system was varied along the axis of the superconductor coil: the center of the pick-up coil system, whose z coordinate is denoted with z_0, agreed with and was 120 mm apart from the center of the superconductor coil.

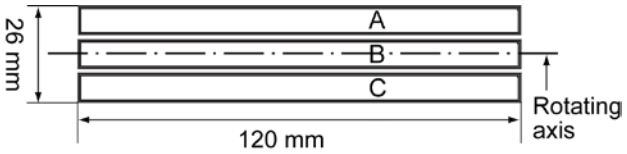

Fig. 2. Schematic of the rotating pick-up coil system. It consists of three pick-up coils. The coils A and B are connected in series so as to cancel the dipole component. The coil C is used independently.

B. Theoretical Method

The magnetic field harmonics were calculated by assuming the line currents at the designed wire positions at the straight section (2D analyses). However, since the constructed coil is relatively short, considering its bore radius, the magnetic field harmonics obtained from the output of pick-up coils could not agree with the theoretical values by the 2D analyses, even if there is no position error of wire.

In addition to the 2D analyses, 3D analyses were carried out as follows. First, based on the designed position of wire as shown in Fig. 1(b), the 3D mapping of the magnetic field generated by the coil current was calculated by using an in-house code based on Biot-Savart's law. Second, the output voltage of the pick-up coil was calculated from the 3D mapping of the magnetic field. Finally, the magnetic field harmonics were calculated from the calculated output of the pick-up coil in a same way as the data analyses of experiments.

In Fig. 3, the magnetic field harmonics by the 2D analyses and those by the 3D analyses are compared with each other, when the coil is wound to its tenth layer. The reference radius is 40 mm. It should be noted that the wire positions are not optimized in its ten layers to suppress higher harmonics. The differences between the 2D analyses and the 3D analyses are small in the sextupole component, whereas they are larger in the decapole component. The magnetic field harmonics by the 3D analyses differ from those by the 2D analyses more at z_0 = 120 mm than at z_0 = 0 mm, due to the influence of the coil end.

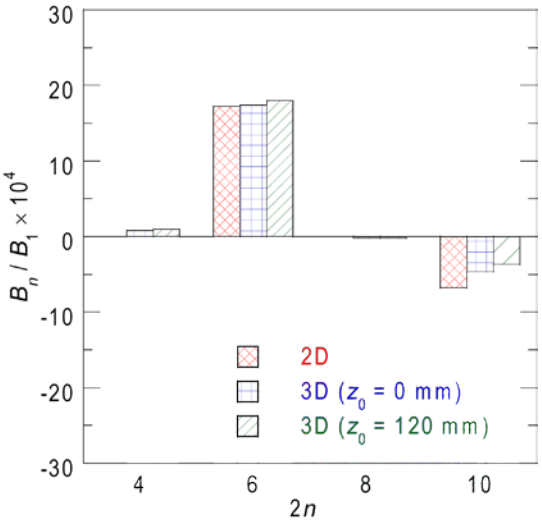

Fig. 3. Magnetic field harmonics by the 2D analyses and those by the 3D analyses.

IV. Results and Discussion

For all data of magnetic field harmonics in this paper, the reference radius is 40 mm. At each condition, the pick-up coils were rotated four times to obtain four cycles of waveform, and, then, the magnetic field harmonics were calculated at each cycle. The average values of the harmonics are shown in the figure, and the error bars are the standard deviation of the four data. Each normal component B_n or skew component A_n is normalized by the normal dipole component B_1 and is multiplied by 10^4.

In Figs. 4 and 5, the magnetic field harmonics measured after winding the twenty-fourth layer (the last layer) are compared with the 3D analyses: Fig. 4 is at z_0 = 0 mm, and Fig. 5 is at z_0 = 120 mm. When looking at the quadrupole and sextupole components, in which the errors of the measured values (error bars) are relatively small, the difference between the measured magnetic field harmonics and the theoretical values are less than 5×10^{-4} at z_0 = 0 mm in Fig. 4. Meanwhile, at z_0 = 120 mm, the difference between the measured sextupole and the calculated one is much larger in Fig. 5(a). When z_0 = 0 mm, the measured harmonics should be dominated by the current (wire positions) in the straight section of the coil, whereas they are influenced more substantially by the current (wire positions) at the coil end. Some position errors of wires were observed visually at the coil end. They should have caused large error in the sextupole component at z_0 = 120 mm.

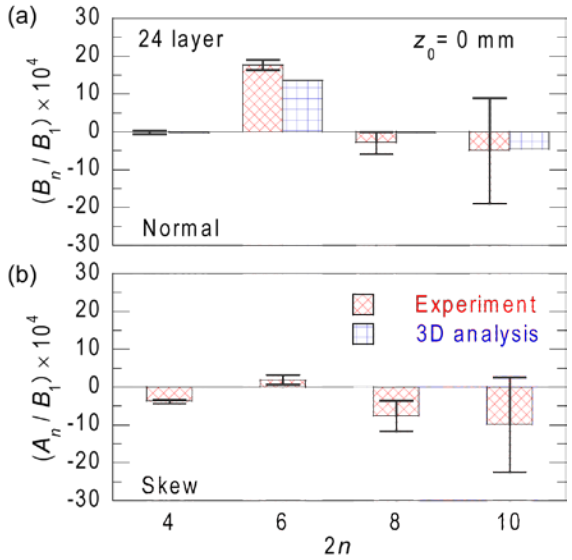

Fig. 4. Magnetic field harmonics measured after winding the twenty-fourth layer and theoretical values by 3D analyses at z_0 = 0 mm.

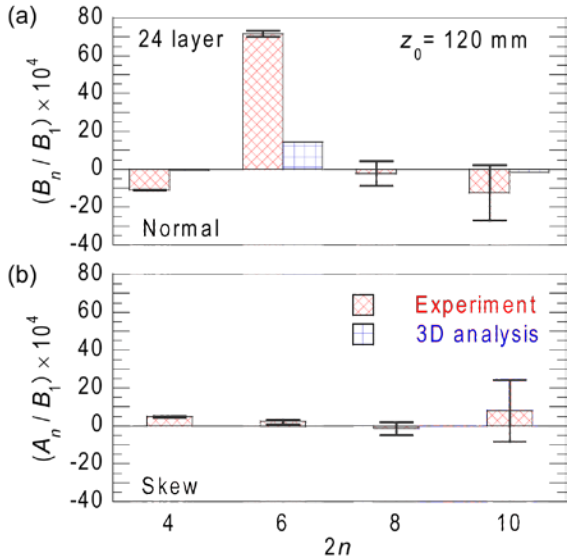

Fig. 5. Magnetic field harmonics measured after winding the twenty-fourth layer and theoretical values by 3D analyses at z_0 = 120 mm.

We define the relative errors in multi-pole component ε as

$$\varepsilon = \left(B_{n,\mathrm{mes}}/B_{1,\mathrm{mes}} - B_{n,\mathrm{cal}}/B_{1,\mathrm{cal}}\right)\times 10^4 : \text{for the normal,} \quad (1)$$

$$\varepsilon = \left(A_{n,\mathrm{mes}}/B_{1,\mathrm{mes}}\right)\times 10^4 : \text{for the skew,} \quad (2)$$

where $B_{n,\mathrm{mes}}$ and $A_{n,\mathrm{mes}}$ are the measured components, and $B_{n,\mathrm{cal}}$ is the calculated component by the 3D analysis, respectively.

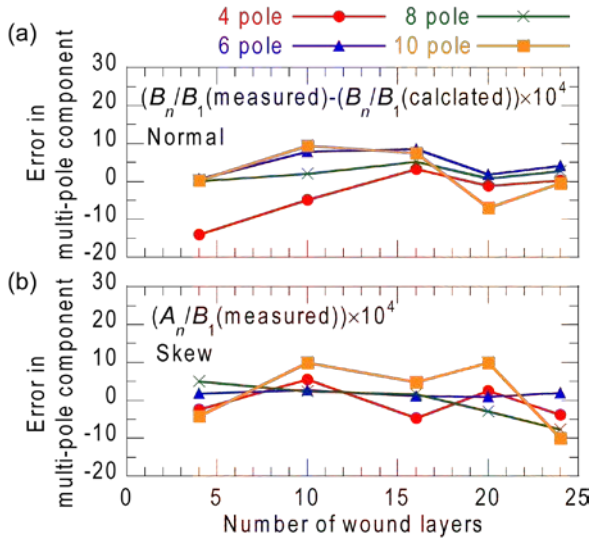

Fig. 6. Relative errors in multi-pole component at z_0 = 0 mm plotted against number of wound layers.

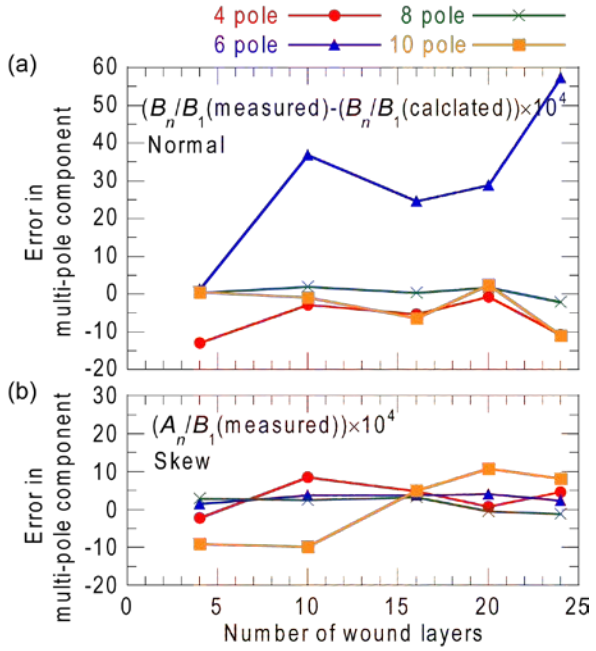

Fig. 7. Relative errors in multi-pole component at z_0 = 120 mm plotted against number of wound layers.

In Figs. 6 and 7, the errors are plotted against the number of wound layers: Fig. 6 is at z_0 = 0 mm, and Fig. 7 is at z_0 = 120 mm. In Fig. 6, no accumulation of the error is observed at z_0 = 0 mm, whereas in Fig. 7(a), the error of the normal sextupole component z_0 = 120 mm increases with increasing number of wound layers. As pointed out in a previous section, visually-observed position errors of wire near the coil end should have accumulated and have caused this error.

The outer dimension of the coil can be measured by contacting the coil with the head of the winding machine, The measurements were carried out at five axial locations (z = -230 mm, -100 mm, 0 mm, 100 mm, 230 mm) and at eight azimuthal locations A–H with the separation of 45 degrees. The locations of z = -100 mm, 0 mm, and 100 mm are in the straight section of the coil, and the locations of z = -230 mm and 230 mm are in the coil end. C and G agree with the poles. Figs. 8(a) and 8(b) show the dimensions after winding respectively the fourth and the twenty-fourth layers. The standard deviation of dimensions at the straight section is 0.078 mm in Fig. 8(a) and is 0.250 mm in Fig. 8(b), respectively.

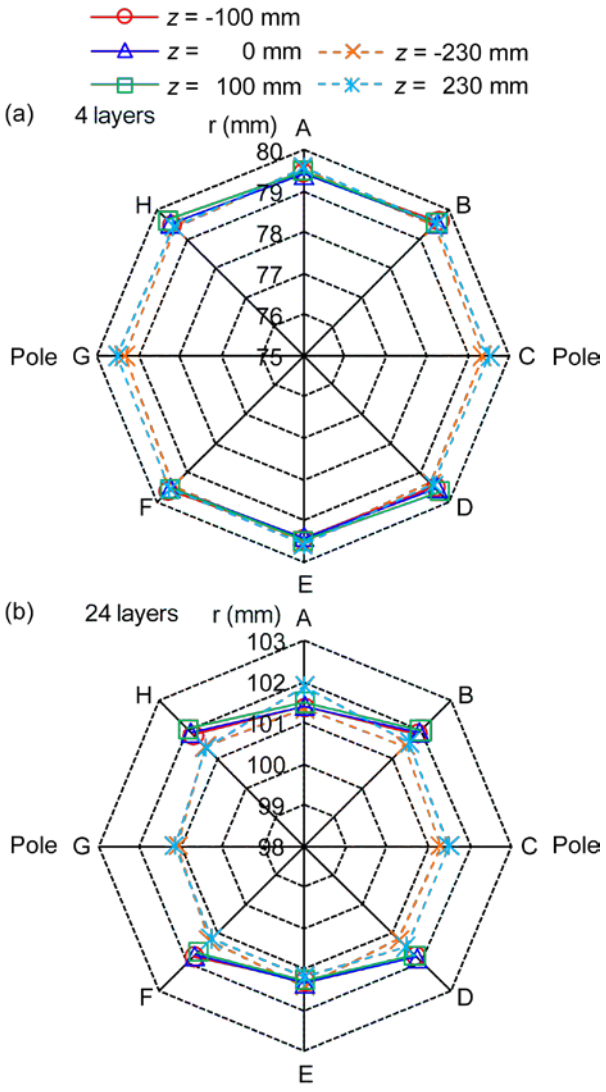

Fig. 8. Measured outer dimensions of coils: (a) after the fourth layer was wound and (b) after the twenty-fourth layer was wound.

In Fig. 8(b), smaller dimensions are observed near the mid plane (A, E) at z = -100 mm, 0 mm, and 100 mm after winding the twenty-fourth layer. This may cause the larger measured normal sextupole components than ones calculated by the 3D analysis.

V. Summary

When the coil was wound to its 24 layers, the difference between the quadrupole, sextupole, octupole, and decapole components calculated from the designed wire positions and those measured magnetically at the center of the coil were less than around 5×10^{-4}. This difference can be used as a measure of the magnetic field error of the winding technology. Generally speaking, the acceptable field error in magnets for circular accelerators is around 1×10^{-4}, whereas that in magnets for high energy beam transport lines, in which a particle passing through only once, is one order of magnitude lager. The current technology reaches a level applicable to the latter with respect to the straight section of magnet. Meanwhile, when the magnetic measurements were carried out at the position 120 mm apart from the center, we observe a larger difference between the calculated and the measured normal sextupole components. Visually-observed position errors of wire near the coil end should have caused this difference. The improvement is more required at this point. Smaller measured dimensions near the mid plane of the coil might cause larger measured normal sextupole components than the calculated ones.

Acknowledgment

N. Amemiya and S. Mizuta thank H. Otake in their group for his assistance when carrying out experiments. N. Amemiya thanks T. Ochi, M. Nii, and K. Takahashi in his group for their cooperation for preparing this paper.

References

[1] S. Russenschuck, *Field computation for accelerator magnets*. Weinheim: WILEY-VCH, 2010, pp. 293–326.

[2] T. Obana *et al.*, "Prototype superconducting magnet for the FFAG accelerator," *Fusion Engineering and Design*, vol. 81, 2006, pp. 2541–2547.

[3] T. Obana *et al.*, "Development of a prototype superconducting magnet for the FFAG accelerator," *IEEE Trans. Appl. Supercond.*, vol. 16, no. 2, pp. 216–219, Jun., 2006.

[4] B. Parker and J. Escallier, "Serpentine coil topology for BNL direct wind superconducting magnets," in *Proc. 2005 Particle Accelerator Conf.*, Knoxville, 2005, pp. 737–739.

[5] P. Wanderer *et al.*, "Completion of superconducting magnet production at BNL for the HERA luminosity upgrade," *IEEE Trans. Appl. Supercond.*, vol. 12, no. 1, pp. 305–308, Mar., 2002.

[6] B. Parker *et al.*, "HERA luminosity upgrade superconducting magnet production at BNL," *IEEE Trans. Appl. Supercond.*, vol. 11, no. 1, pp. 1518–1521, Mar., 2001.

[7] T. Obana *et al.*, "Magnetic field design of superconducting magnet for a FFAG accelerator," *IEEE Trans. Appl. Supercond.*, vol. 15, no. 2, pp. 1185–1188, Jun., 2005.

[8] N. Ohuchi, K. Tsuchiya, M. Tawada, N. Higashi, M. Iwasaki, and Z. Zong, "Design and construction of the final focus quadrupole R&D magnet for super-KEKB," *IEEE Trans. Appl. Supercond.*, vol. 21, no. 3, pp. 1829–1832, Jun. 2011.